Chemistry–A European Journal
Research Article
doi.org/10.1002/chem.202104227
Chemistry Europe
European Chemical Societies Publishing
www.chemeurj.org

Kinase Sensing Based on Protein Interactions at the Catalytic Site

Ohad Solomon,[a] Hannah Sapir,[a] Evgeniy Mervinetsky,[a] Yu-Ju Chen,[b] Assaf Friedler,*[a] and Shlomo Yitzchaik*[a]

Abstract: The role kinases play in regulating cellular processes makes them potential biomarkers for detecting the onset and prognosis of various diseases, including many types of cancer. Current kinase biosensors, including electrochemical and radiometric methods, rely on sensing the ATP-dependant enzymatic phosphorylation reaction. Here we introduce a new type of interaction-based electrochemical kinase biosensor that does not require any chemical labelling or modification. The basis for sensing is the interactions between the catalytic site of the kinase and the phosphorylation site of its substrate rather than the phosphorylation reaction. We demonstrated this concept with the ERK2 kinase and its substrate protein HDGF, which is involved in lung cancer. A peptide monolayer derived from the HDGF phosphorylation site was adsorbed onto a gold electrode and was used to sense ERK2 without ATP. The sensitivity of the assay was down to 10 nM of ERK2, corresponding with the range of its cellular concentrations. Surface chemistry analysis confirmed that ERK2 was bound to the HDGF peptide monolayer. This increased the permeability of redox-active species through the monolayer and resulted in ERK2 electrochemical sensing. Since our detection approach is based on protein-protein interactions and not on the enzymatic reaction, it can be further utilized for more selective detection of different types of enzymes.

Introduction

Kinases are key components in regulating numerous key cellular processes, including cell growth and proliferation.[1] Accordingly, abnormal kinase activity is closely connected to many diseases, including various types of cancer[2] and kinases are considered to be promising cancer biomarkers.[3,4] Many analytical methods have been developed for kinase activity quantification as prognostic tools,[5,6] including radiometric,[7,8] spectroscopic[9–11] and immunological tools.[12,13] Electrochemical methods were also developed for kinase detection,[14–18] and as all electrochemical tools they have the distinct advantages of relatively low cost, easy operation, rapid response and high sensitivity.[19] Though each of these different detection tools is unique in its method of operation, they all share a dependance on the enzymatic phosphorylation reaction in the presence of ATP, which is necessary for sensing. The kinase ERK2 is the most down-stream kinase in the MAPK/ERK pathway and is involved in regulating a variety of cellular processes, including differentiation, proliferation, stress responses and apoptosis.[20] Specifically, ERK2 is responsible for phosphorylating and activating many transcription factors that promote gene expression, and is closely related to the development of various types of cancer.[21] We have previously shown that ERK2 is responsible for the overphosphorylation of the Hepatoma-derived growth factor (HDGF) protein at Ser165 in non-small-cell lung carcinoma (NSCLC).[22] HDGF is a mitotic factor, involved in the growth process of vascular smooth muscle cells, hepatoma cells and endothelial cells,[23] and when overexpressed in adults is considered a biomarker for various diseases.[24] Based on this kinase-substrate pair, a label-free electrochemical kinase biosensor was previously developed in our labs.[22,25]

Sensing based on the catalytic activity of an enzyme, phosphorylation in the case of ERK2, has the major disadvantage of low specificity. This is because many kinases share common phosphorylation sites and thus phosphorylate the same sequences within a given protein. A way to overcome the lack of selectivity in sensing is to use protein interactions, which are much more specific, rather than catalytic activity. We have demonstrated this approach for sensing based on interactions of the kinase at the docking site, which is distant from the catalytic site.[26] Here we show that sensing can also be performed based on the inherent protein interactions between the catalytic site of the kinase and the phosphorylation sequence of the substrate, but without ATP. We demonstrated this concept with a new type of an electrochemical ERK2 biosensor. For this purpose, we developed an assay comprised of a peptide derived from the phosphorylation site of HDGF, adsorbed onto a gold electrode. To ensure that no phosphor-

[a] O. Solomon, H. Sapir, Dr. E. Mervinetsky, Prof. A. Friedler, Prof. S. Yitzchaik
Institute of Chemistry and the Center for Nanoscience and Nanotechnology
The Hebrew University of Jerusalem
Safra Campus, Givat Ram, Jerusalem, 91904 (Israel)
E-mail: assaf.friedler@mail.huji.ac.il
shlomo.yitzchaik@mail.huji.ac.il

[b] Prof. Y.-J. Chen
Institute of Chemistry
Academia Sinica
No. 128, Section2, Academia Road, Taipei, 115 (Taiwan)

Supporting information for this article is available on the WWW under https://doi.org/10.1002/chem.202104227

ylation could occur and that sensing was not phosphorylation-based, the exposure of the assay to ERK2 was performed in the absence of ATP. The electrochemical response was monitored using electrochemical impedance spectroscopy (EIS), which does not require any labelling or chemical modifications, before and after exposure to the kinase ERK2.

Results and Discussion

Peptide design

A peptide derived from the HDGF phosphorylation site, residues 160–174, was synthesized with a CGGG sequence at its N-terminus. The Cysteine residue was added for binding to gold surfaces, while the three Glycine residues were added as a spacer to decouple the phosphorylation site from the electrode surface, allowing the peptide to adopt a more native conformation. In addition, a Tryptophan residue was added at the C-terminus of the peptide to allow accurate concentration measurement using UV-Vis spectrophotometry. The final sequence of the peptide, termed herein as the "HDGF peptide", is CGGG^{160}DLLEDSPKRPKEAEN^{174}W.

Electrochemically sensing ERK2 in the absence of ATP

Electrochemical impedance spectroscopy (EIS) was used to monitor peptide monolayer assembly and ERK2 detection. The HDGF peptide was adsorbed onto gold macroelectrodes, which according to EIS measurements, resulted in a significant increase in the resistance to charge transfer (R_{CT}) through the layer from 70 Ω to 6,250 Ω (Figure 1A). This increase is due to the formation of a peptide monolayer on the electrode, which acts as an insulating layer and decreases the permeability of the redox-active species, the electron carriers in this system, to the surface of the electrode. The modified electrodes were then exposed to ERK2, which resulted in a significant decrease in R_{CT} values (Figure 1A) to 359 Ω, due to an increase in the permeability of the redox-active species. These results were fit with the Randles circuit, $R_S[(R_{CT}W)||Q]$ (see inset to Figure 1B), where R_s is the resistance of the solution, R_{CT} is the resistance to charge transfer, W is the Warburg element representing the diffusion-controlled resistance and Q is a constant phase element, which describes a nonideal capacitor and replaces the double-layer capacitor.[27]

To determine whether the changes in R_{CT} values after exposure to ERK2 were indeed due to ERK2 and not to components of the buffer or to non-specific interactions, we repeated this experiment with the kinase buffer as control (Figure 1B). To determine the selectivity of the assay towards ERK2, we also performed these experiments with Bovine serum albumin (BSA), the MAPK p38γ and the kinases PKCδ and CDK5 in place of ERK2 (Figure 1B). In these experiments the relative R_{CT} is defined as the R_{CT} value before the exposure of the electrode to ERK2 divided by the R_{CT} value after exposure to ERK2. The electrodes exposed to the control buffer, BSA and

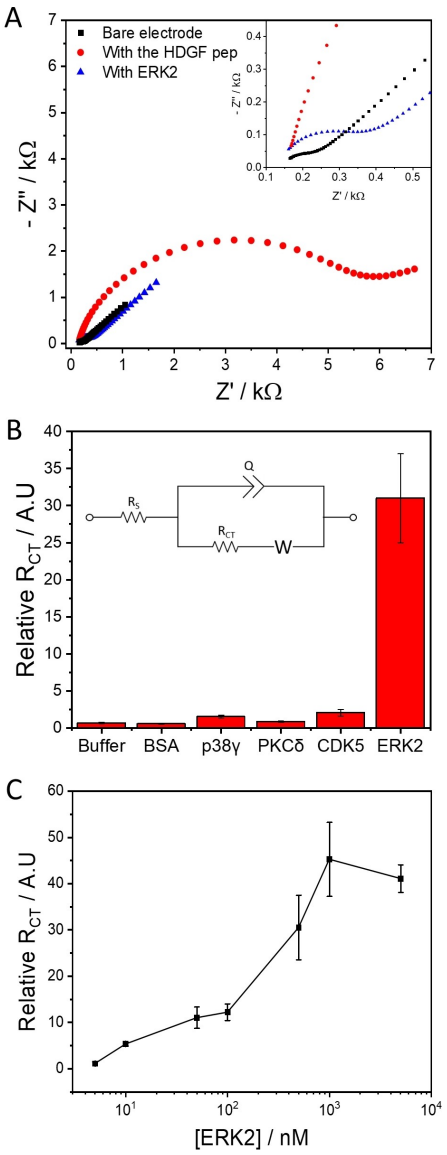

Figure 1. Electrochemical characterization of the essay using EIS. (A) Adsorption of the HDGF peptide resulted in a significant increase in R_{CT} values (■→●) from 70 Ω to 6,250 Ω as a result of the peptide layer formation. Exposure to ERK2 resulted in a significant decrease in R_{CT} values (●→▲) from 6,250 Ω to 314 Ω; (B) Control and selectivity experiment, using the kinase buffer and 0.5 μM BSA, p38γ, PKCδ and CDK5 to verify the selectivity of the assay towards ERK2; (C) Dose-response experiments revealed that the sensitivity of the assay is in the range of 10 nM–10 μM.

PKCδ showed no significant increase in R_{CT} values. Though the responses to p38γ and CDK5 were more significant, they were 15 to 20-fold lower than the response to ERK2. We assume that this is due to the difference in affinities of the inappropriate kinases compared with ERK2 towards the HDGF substrate peptide, confirming that the electrochemical response of the assay is due to specific interactions and is indeed selective towards ERK2.

Next, we evaluated the sensitivity of the assay by exposing it to different ERK2 concentrations, ranging from 5 nM to 5 μM (Figure 1C). The dose response experiment revealed that the

assay is sensitive for ERK2 concentrations between 10 nM and 1 μM, with a limit of detection (LOD) of 8.1 nM and a limit of quantification (LOQ) of 27 nM (for detailed calculations see Supporting Information).[28] This range correlates with the cellular concentration of ERK2 (50 nM–2 μM, depending on its cellular location).[29]

Surface chemistry analysis showed that ERK2 is adsorbed onto the HDGF peptide monolayer

To determine the changes in the peptide monolayer after exposure to ERK2 and to understand the mechanism of electrochemical sensing we used surface chemistry analysis.

X-ray photoelectron spectroscopy (XPS) analysis was performed for elemental analysis of the monolayer-modified gold substrates before and after exposure to ERK2. These measurements revealed indicative peaks at binding energies of 285.2, 286.4 and 288.3 eV, corresponding with C 1s C–H, C–O/C–N and C=O moieties, respectively (Figure 2A), and 400.1 eV (Figure 2B), corresponding with the N 1s C–N moiety.[30] This serves as evidence for the successful adsorption of the HDGF peptide on the gold surfaces. We assume that the peak at 285.2 eV present in the spectra of the bare gold substrates indicates the presence of carbon impurities. Exposure of the HDGF peptide-modified surfaces to ERK2 resulted in a significant increase in the peaks described above (Figure 2), suggesting that ERK2 was bound to the peptide monolayer.

Variable angle spectroscopic ellipsometry (VASE) measurements showed that while the theoretical length of the HDGF peptide is 25–30 Å, the optical thickness of the peptide monolayer was 15 ± 3 Å. This could be the result of partial coverage and/or of tilted alignment of the peptides in the layer. Another explanation is that the conformation of the peptide is not linear, but has some residual structure, as can be seen from the minimum at 203 nm in the circular dichroism (CD) spectrum of the peptide (Figure 3A), corresponding with β-turns.[31] This can be explained by the presence of the two Proline residues roughly at the middle of the sequence, which are known to induce β-turns.[32] After exposure to ERK2 the optical thickness of the organic layer increased to 26 ± 3 Å, which again indicates the binding of ERK2 to the HDGF peptide monolayer. The change in the layer thickness after exposure to ERK2, 10 ± 3 Å, is smaller than the ERK2 theoretical radii, 20 to 30 Å, calculated using the PyMOL software and the 2FYS PDB file.[33] Since ellipsometric data is averaged over the total irradiated area, we assume that the coverage of the ERK2 layer on top of the peptide layer is only partial, explaining the difference between the experimental additional optical thickness and the ERK2 calculated radii.

Polarization modulation infrared reflection-absorption spectroscopy (PM-IRRAS) measurements were performed to determine the orientation of the functional groups in the HDGF peptide monolayer (Figure 3B), which could indicate conformational changes in the HDGF peptide monolayer. In this method, the intensity represents the subtraction of the s-polarization,

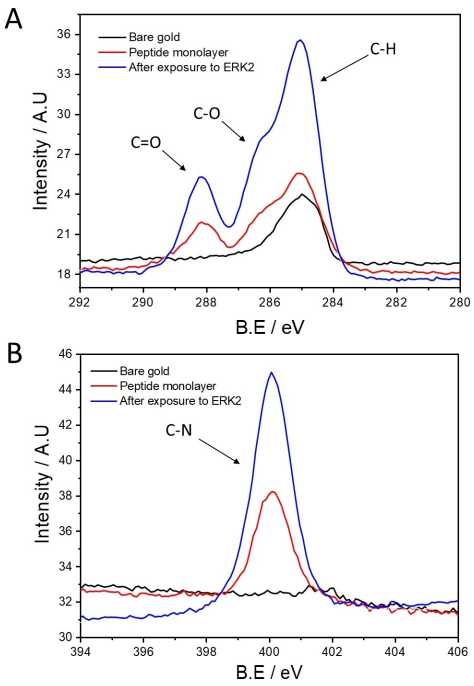

Figure 2. XPS analysis of the HDGF peptide and ERK2-modified surfaces suggests the binding of ERK2 to the HDGF peptide monolayer. (A) Analysis of C 1s; (B) Analysis of N 1s. The significant increase in intensity after exposure to ERK2 suggests the binding of ERK2 to the HDGF peptide monolayer.

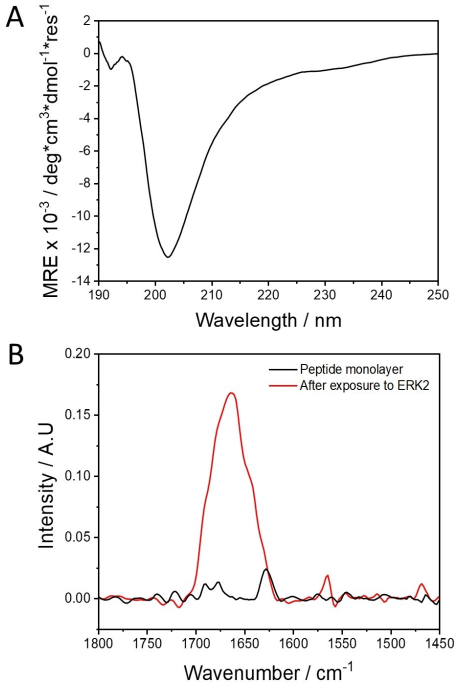

Figure 3. (A) The CD spectrum of the HDGF peptide in PBS showed that the HDGF peptide adopts a β-turn structure, as can be seen by the minimum at 203 nm; (B) PM-IRRAS measurements revealed an increase in the absorbance at the amide I region, which may be the result of both the binding of ERK2 to the peptide monolayer and conformational changes in the layer.

parallel to the surface, from the p-polarization, perpendicular to the surface. The results show a significant change in absorbance of the amide I region (1620–1750 cm^{-1}), corresponding with C=O stretching and N–H in-plane bending, after exposure to ERK2.[34] Since the amide I region is usually sensitive to conformational changes,[35] the increase in absorbance could be due to a combination of the presence of additional functional groups, as a result of the binding of ERK2 to the peptide monolayer, as well as conformational changes in the HGDF peptide monolayer.

Atomic force microscopy (AFM) analysis was performed to determine the changes in the topography of the HDGF peptide layer after exposure to ERK2. The results showed that the adsorption of the HDGF peptide only slightly increased the average surface roughness (Ra) compared to bare gold (Figures 4A and B), suggesting the formation of a homogeneous peptide layer. On the other hand, after exposure to ERK2 the surface seemed rougher and disordered, which was manifested by a significant increase in the average surface roughness, from 0.25 ± 0.08 nm to 0.83 ± 0.03 nm (Figures 4B and C). We suggest that this change is due to the binding of ERK2 to the HDGF peptide layer that changed the packing of the layer from homogeneous and dense to disordered. This also explains the increased permeability of the redox-active species observed in the electrochemical measurements.

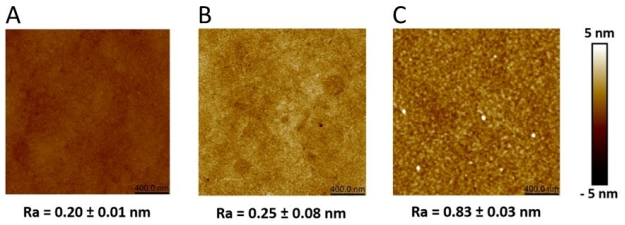

Figure 4. AFM analysis and surface roughness measurements of the modified gold substrates. (A) Bare gold; (B) after adsorption of the HDGF peptide; (C) after incubation with ERK2. The increase in surface roughness after the exposure to ERK2 suggests that its binding to the peptide monolayer resulted in a rearrangement of the layer from ordered and dense to disordered.

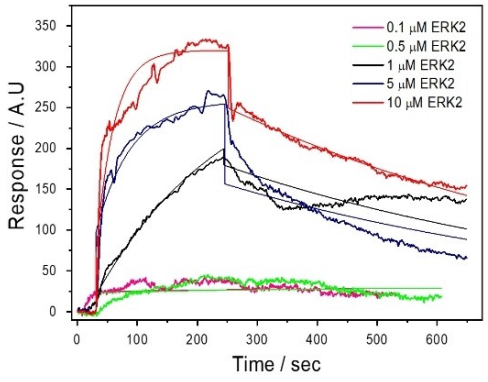

Figure 5. Sensorgrams of SPR on-surface binding experiments between ERK2 and the HDGF peptide. Exposure to various concentrations of ERK2, ranging between 0.1 μM–10 μM, showed that the binding in concentration-dependent and that the association phase reaches equilibrium much faster than the dissociation phase.

Surface plasmon resonance (SPR) was used to quantify the on-surface kinetics and interactions between ERK2 and the surface-bound HDGF peptide (Figure 5). These experiments showed that ERK2 bound the HDGF peptide in a concentration-dependant manner, corresponding with the sensitivity revealed in the EIS dose response experiments. The system reached equilibrium rapidly during the association phase, $k_a = (3.2 \pm 0.2) \cdot 10^3\ M^{-1} \cdot sec^{-1}$, while equilibrium in the dissociation phase was achieved much slower, $k_d = (1.4 \pm 0.2) \cdot 10^{-3}\ sec^{-1}$. This supports our hypothesis that after the binding of ERK2 to the HDGF peptide monolayer, repeated washes did not remove it, and that sensing is indeed a result of ERK2 binding. In addition, we were able to determine the K_D of the interaction to be 0.44 ± 0.02 μM, which suggests a strong interaction between ERK2 and the HDGF peptides in the monolayer.

Conclusions

The development of analytical methods for detection of enzymes, and specifically kinases, is crucial for the diagnosis of diseases and is an essential step for future therapy. In this work we demonstrated a new approach for selective kinase sensing, based on the interaction between the catalytic site of the kinase ERK2 and the phosphorylation sequence of its substrate HDGF, rather than on the traditional catalytic phosphorylation of the substrate. We were able to monitor the changes in the HDGF peptide monolayers electrochemically using EIS and determined the sensitivity of the assay to be in the range of 10 nM–1 μM. To understand the molecular mechanism of sensing, we performed surface analysis. XPS, VASE and PM-IRRAS showed that after exposure of the assay to ERK2 a binding event occured and ERK2 was anchored to the HDGF peptide monolayer. AFM revealed that this binding event changed the morphology of the layer from homogeneously smooth to inhomogeneous and rough. According to these results, we suggest that as a result of the binding of ERK2, the peptide layer undergoes rearrangement in a way that makes it permeable to the redox-active species, enabling them to reach the surface of the electrode and resulting in the electrochemical sensing of ERK2.

While some previously reported kinase biosensors exhibited higher sensitivity and sometimes even a larger sensitivity range,[15,36] our assay has the distinct advantage of being highly selective, fast to use and requires no further analysis. In addition, while many biosensors require multistep assembly, our biosensor, only requires the simple and standard thiol-mediated adsorption on gold surfaces in a single step, making it highly versatile. Both previous and current kinase sensing methods require the use of radio-labelled ATP.[8] This derivative is expensive, requires immediate use and raises unnecessary health risks. Other detection methods require the use of either ferrocene-[17] or fluorophore-labelled[37–39] ATP for detection of the phosphorylation reaction. Though our assay is not completely label free, due to our use of the Ferri/Ferrocyanide redox

couple as electron carriers, it does not require any chemical labelling or modifications, making it easier and generally cheaper to use. Label free methods for kinase sensing, including ELISA, use the specific interactions between antibodies and kinases or the product phosphoproteins.[40,42] While these methods are sensitive and highly specific, the antibodies are also expensive and require tedious and time-consuming handling procedures. Furthermore, ELISA is only a semi-quantitative method, while our method is quantitative. Previous research in our labs showed that the enzymatic selectivity of kinases usually decreases over time. This is due to the fact that, if given enough time, kinases will eventually phosphorylate non-specific substrates, resulting in the loss of selectivity.[18] In the assay described herein, on the other hand, since the sensing is interaction-based and not phosphorylation-based, the selectivity should remain over time. We recently showed that sensing ERK2 can also be achieved by exploiting the protein-protein interactions between ERK2 and its substrate ELK1 at the docking site of ERK2.[26] These two directions can be used together as a new integrative approach for selective kinase sensing.

In conclusion, our new concept for kinase sensing that harnesses the interactions between the kinase and its substrate at the catalytic site, can be further utilized for detecting different kinases and types of enzymes in a selective manner by changing the surface-bound peptide. Sensing a specific enzyme can also be done by using different peptides to target different sites of the analyte, such as the active and docking sites.

Experimental Section

Peptide synthesis and purification: The peptides were synthesized on a Liberty blue microwave assisted peptide synthesizer (CEM) using a standard fluorenylmethyloxycarbonyl chloride (Fmoc) chemistry and N,N′-diisopropylcarbodiimide (DIC) / ethyl cyanohydroxyiminoacetate (Oxyma) as coupling reagents. For SPR on-surface binding experiments some of the peptide, still on resin, was labelled with Biotin at the N-termini. For that purpose, 50 mg of the resin were added to a solution of 53 μL DIEA, 64 mg PyBOP and 30 mg biotin dissolved in 2 mL DMF. The solution was shaken for 16 h at room temperature, following washes of the resin with DMF, DCM and methanol. The peptides were cleaved from the resin as described.[43] Purification of the peptides was done on a MERCK-Hitachi semi-preparative HPLC using a reverse-phase Waters C18 semi-preparative column with a gradient of MeCN/TDW. The identity and purity of the peptides were determined using an electrospray ionization (ESI) mass spectrometry and an analytical MERCK-Hitachi HPLC, respectively.

Protein expression and purification: The constitutively active mutant of ERK2 (R65S)[44] was expressed using a NpT7-5 His6-ratERK2 plasmid, courtesy of Prof. Oded Livnah (The Alexander Silberman institute of life sciences, The Hebrew University of Jerusalem). Expression of the protein was carried out as described.[45] The protein contains six His residues at its N-terminus for affinity purification. After expression, the bacteria were suspended in the lysis buffer (containing 25 mM Tris-HCl pH = 8.0, 500 mM NaCl, 5% glycerol, 5 mM β-mercaptoethanol, 300 mM imidazole and a cocktail of protease inhibitors) and lysed using a microfluidizer. The soluble fraction was separated by centrifugation and loaded on a nickel Sepharose 4 mL column. Elution of the protein was performed using an imidazole gradient, at 100% elution buffer (containing 25 mM Tris-HCl pH = 8.0, 500 mM NaCl, 5% glycerol, 5 mM β-mercaptoethanol and 300 mM imidazole). The protein was further purified using a size-exclusion Sephacryl S100 500 mL column. Elution was performed using a buffer containing 25 mM Tris-HCl pH = 8.0, 300 mM NaCl, 5% glycerol and 0.5 mM β-mercaptoethanol, which was also used as the storage buffer. The purification process of $ERK2^{R65S}$ was carried out on an Äkta Explorer FPLC system, and the protein purity was confirmed by Coomassie staining of SDS-PAGE gel.

Gold electrode preparation and modification: Polycrystalline bulk gold electrodes with 2 mm diameter (CH Instruments, USA) were polished using a slurry of 0.05 μm alumina for 1 min, and were then thoroughly washed with TDW and sonicated in a 1:1 solution of ethanol and TDW, to remove any excess alumina. After electrochemically verifying the cleanness of the electrodes, a 70 μL peptide solution (10 μM) was dropped on the surface of the gold macroelectrodes, and these were incubated for 16 h at 16 °C. The electrodes were then rinsed 3 times in TDW. The peptide solution was prepared by dissolving the peptide in a slightly basic solution (1 equiv. of 100 mM sodium bicarbonate and 21 equiv. of TDW). The reaction with the kinase ERK2 was performed by dropping a 40 μL freshly-prepared kinase solution (5 nM–5 μM) on the surface of the modified electrodes, which were then incubated for 30 mins at 37 °C. The reaction medium was 80 mM Tris-HCl pH = 7.5 and 40 mM $MgCl_2$. The electrodes were then rinsed 3 times in TDW.

Gold surface preparation and modification: The surfaces were washed with ethanol, dried under a mild stream of nitrogen gas and cleaned using UVOCS (ultraviolet ozone cleaning system) for 20 min. A 150 μL peptide solution (100 μM), prepared as described above, was then dropped on the surfaces and these were incubated for 16 h at 16 °C. The surfaces were then rinsed 3 times in TDW and dried under a mild stream of nitrogen gas. The reaction with ERK2 was performed by dropping a 150 μL kinase solution (3 μM) on the surfaces, which were then incubated for 30 min at 37 °C. The surfaces were then rinsed 3 times in TDW and dried under a mild stream of nitrogen gas.

Electrochemical characterization: Electrochemical measurements were taken following each surface modification step. EIS measurements were performed using a Bio-Logic SP-300 potentiostat (Bio-Logic Science Instruments) connected to an EC-LAB software package. A conventional three-electrode cell was employed with the modified gold electrode as working electrode, a Pt counter electrode and a standard Ag/AgCl reference electrode (Metrohm) with 3 M KCl. EIS measurements were carried out in a solution containing 5 mM of the redox-active species, $K_3[Fe(CN)_6]$ and $K_4[Fe(CN)_6]$ and 0.1 M KCl as a supporting electrolyte. The spectra were recorded at a frequency range of 0.1 Hz–10 kHz with an amplitude of 10 mV, at the formal potential of E = 0.21 V (vs. Ag/AgCl electrode).

X-ray photoelectron spectroscopy (XPS) analysis was performed using a monochromatic Al Kα X-ray source on a Kratos AXIS ULTRA instrument.

Variable angle spectroscopic ellipsometry (VASE) measurements were performed with a VB-400 (Woollam Co.) ellipsometer at the Brewster angle of 75°.

Circular dichroism (CD) spectra of the HDGF peptide were recorded with a J-810 spectropolarimeter (JASCO) equipped with a Peltier thermostat and running the supplied Spectra Manager software. Samples were placed in 0.1 cm quartz cuvettes for far-UV CD spectroscopy and scanned in the spectral range 190–260 nm. The peptides were tested in PBS and in TDW.

Polarization modulation infrared reflection absorption spectroscopy (PM-IRRAS) measurements were performed at room temperature under positive nitrogen gas pressure on a reflection-absorption cell (Harrick, Inc.) with a PMA-50 PM-FTIR spectrometer coupled to a Vertex V70 (Bruker). The signal was collected from the modified gold surfaces by

2048 scans with a resolution of 4 cm^{-1} using a mercury cadmium telluride detector.

Atomic force microscopy (AFM) analysis was performed using a Dimension Icon XR probe microscope (Bruker) in tapping mode.

Surface plasmon resonance (SPR) analysis was performed using an OpenSPR 2-Channel Starter Pack (R4.2) biosensor system (Nicoya). For this analysis, Biotin-streptavidin sensor chips were used. Following running buffer equilibration (containing 25 mM Tris pH = 8, 100 mM NaCl and 0.5 mM β-mercaptoethanol), streptavidin immobilization was performed until a stable signal was achieved. In the ligand immobilization step, 25 μM N-terminus biotinylated HDGF peptide was injected until a stable signal was achieved. Injections of the analyte, ERK2, were performed in a range of concentrations (0.1–10 μM). After each analyte injection a regeneration step followed, performed by injecting 10 mM HCl. Both ligand and analyte were diluted in the running buffer.

Acknowledgements

AF and SY thank the support of the Israel Science Foundation (ISF) grant number 1628/18. This work was supported by the Academia Sinica and the Hebrew University of Jerusalem joint research program in Nanoscience and Nanotechnology and The Minerva Center for Bio-Hybrid complex systems. S.Y. thanks the Binjamin H. Birstein Chair in Chemistry. AF thanks the Saerree K. and Louis P. Fiedler Chair in Chemistry.

Conflict of Interest

The authors declare no conflict of interest.

Data Availability Statement

The data that support the findings of this study are available from the corresponding author upon reasonable request.

Keywords: biosensing · electrochemical biosensing · kinase sensing · protein-protein interactions · surface chemistry

[1] J. Rauch, N. Volinsky, D. Romano, W. Kolch, *Cell Commun. Signaling* **2011**, *9*, 1–23.
[2] K. S. Bhullar, N. O. Lagarón, E. M. McGowan, I. Parmar, A. Jha, B. P. Hubbard, H. P. V. Rupasinghe, *Mol. Cancer* **2018**, *17*, 1–20.
[3] S. Vicent, J. M. López-Picazo, G. Toledo, M. D. Lozano, W. Torre, C. Garcia-Corchón, C. Quero, J. C. Soria, S. Martín-Algarra, R. G. Manzano, L. M. Montuenga, *Br. J. Cancer* **2004**, *90*, 1047–1052.
[4] L. R. Yu, H. J. Issaq, T. D. Veenstra, *Proteomics Clin. Appl.* **2007**, *1*, 1042–1057.
[5] C. J. Gray, M. J. Weissenborn, C. E. Eyers, S. L. Flitsch, *Chem. Soc. Rev.* **2013**, *42*, 6378–6405.
[6] A. Basso, S. Serban, *J. Mol. Catal.* **2019**, *479*, 1–20.
[7] T. Feilner, C. Hultschig, J. Lee, S. Meyer, R. G. H. Immink, A. Koenig, A. Possling, H. Seitz, A. Beveridge, D. Scheel, D. J. Cahill, H. Lehrach, J. Kreutzberger, B. Kersten, *Mol. Cell. Proteomics* **2005**, *4*, 1558–1568.
[8] K. C. Duong-Ly, J. R. Peterson, *Methods Mol. Biol.* **2016**, *1360*, 87–95.
[9] Y. Han, H. Li, Y. Hu, P. Li, H. Wang, Z. Nie, S. Yao, *Anal. Chem.* **2015**, *87*, 9179–9185.
[10] S. Gupta, H. Andresen, J. E. Ghadiali, M. M. Stevens, *Small* **2010**, *6*, 1509–1513.
[11] A. W. Tai, N. Bojjireddy, T. Balla, *Anal. Biochem.* **2011**, *417*, 97–102.
[12] O. Montecchini, S. Braidotti, R. Franca, G. Zudeh, C. Boni, C. Sorio, E. Toffoletti, M. Rabusin, A. Tommasini, G. Decorti, G. Stocco, *Front. Pharmacol.* **2021**, *12*, 1–10.
[13] A. M. Lipchik, R. L. Killins, R. L. Geahlen, L. L. Parker, *Biochemistry* **2012**, *51*, 7515–7524.
[14] J. Wang, M. Shen, Y. Cao, G. Li, *Biosens. Bioelectron.* **2010**, *26*, 638–642.
[15] Y. Zhou, H. Yin, X. Li, Z. Li, S. Ai, H. Lin, *Biosens. Bioelectron.* **2016**, *86*, 508–515.
[16] K. Kerman, H. B. Kraatz, *Biosens. Bioelectron.* **2009**, *24*, 1484–1489.
[17] H. Song, K. Kerman, H. B. Kraatz, *Chem. Commun.* **2002**, *8*, 502–504.
[18] E. Snir, J. Joore, P. Timmerman, S. Yitzchaik, *Langmuir* **2011**, *27*, 11212–11221.
[19] Q. Hu, J. Kong, D. Han, Y. Zhang, Y. Bao, X. Zhang, L. Niu, *Anal. Chem.* **2019**, *91*, 1936–1943.
[20] Y. Guo, W. Pan, S. Liu, Z. Shen, Y. Xu, L. Hu, *Exp. Ther. Med.* **2020**, *19*, 1997–2007.
[21] M. Costa, M. Marchi, F. Cardarelli, A. Roy, F. Beltram, L. Maffel, G. M. Ratto, *J. Cell Sci.* **2006**, *119*, 4952–4963.
[22] E. Amit, R. Obena, Y.-T. Wang, R. Zhuravel, A. J. F. Reyes, S. Elbaz, D. Rotem, D. Porath, A. Friedler, Y.-J. Chen, S. Yitzchaik, *Chem. Sci.* **2015**, *6*, 4756–4766.
[23] A. Shetty, S. Dasari, S. Banerjee, T. Gheewala, G. Zheng, A. Chen, A. Kajdacsy-Balla, M. C. Bosland, G. Munirathinam, *Urol. Oncol. Semin. Orig. Investig.* **2016**, *34*, 483.e1-483.e8.
[24] S. S. Hsu, C. H. Chen, G. S. Liu, M. H. Tai, J. S. Wang, J. C. Wu, M. L. Kung, E. C. Chan, L. F. Liu, *J. Neuro-Oncol.* **2012**, *107*, 101–109.
[25] R. Zhuravel, E. Amit, S. Elbaz, D. Rotem, Y.-J. Chen, A. Friedler, S. Yitzchaik, D. Porath, *Sci. Rep.* **2016**, *6*, 1–6.
[26] P. Namdev Joshi, E. Mervinetsky, O. Solomon, Y.-J. Chen, S. Yitzchaik, A. Friedler, DOI 10.1101/2021.11.16.468793, https://www.biorxiv.org/content/10.1101/2021.11.16.468793v1.
[27] J. S. Daniels, N. Pourmand, *Electroanalysis* **2007**, *19*, 1239–1257.
[28] B. Çakıroğlu, J. Chauvin, A. Le Goff, K. Gorgy, M. Özacar, M. Holzinger, *Biosens. Bioelectron.* **2020**, *169*, 1–8.
[29] J. E. Ferrell, E. M. Machleder, *Science* **1998**, *280*, 895–898.
[30] J. S. Stevens, A. C. De Luca, M. Pelendritis, G. Terenghi, S. Downes, S. L. M. Schroeder, *Surf. Interface Anal.* **2013**, *45*, 1238–1246.
[31] C. A. Bush, S. K. Sarkar, K. D. Kopple, *Biochemistry* **1978**, *17*, 4951–4954.
[32] A. M. C. Marcelino, L. M. Gierasch, *Biopolymers* **2008**, *89*, 380–391.
[33] S. Liu, J. P. Sun, B. Zhou, Z. Y. Zhang, *Proc. Natl. Acad. Sci. USA* **2006**, *103*, 5326–5331.
[34] A. Barth, *Biochim. Biophys. Acta Bioenerg.* **2007**, *1767*, 1073–1101.
[35] J. Kong, S. Yu, *Acta Biochim. Biophys. Sin.* **2007**, *39*, 549–559.
[36] Z. Zhao, X. Zhou, D. Xing, *Biosens. Bioelectron.* **2012**, *31*, 299–304.
[37] M. Sato, T. Ozawa, T. Yoshida, Y. Umezawa, *Anal. Chem.* **1999**, *71*, 3948–3954.
[38] K. Y. Tomizaki, H. Mihara, *Mol. BioSyst.* **2006**, *2*, 580–589.
[39] F. Sipieter, P. Vandame, C. Spriet, A. Leray, P. Vincent, D. Trinel, J. F. Bodart, F. B. Riquet, L. Héliot, *Prog. Mol. Biol. Transl. Sci.* **2013**, *113*, 145–216.
[40] Y. Sugiyama, I. Kameshita, *Biochem. Biophys. Rep.* **2017**, *11*, 40–45.
[41] D. A. Pena, V. P. De Andrade, G. Á. F. Silva, J. I. Neves, P. S. L. De Oliveira, M. J. M. Alves, L. A. Devi, D. Schechtman, *Sci. Rep.* **2016**, *6*, 1–11.
[42] M. Eto, S. Katsuki, Y. Tanaka, K. Takeya, *BioTechniques* **2020**, *68*, 211–213.
[43] R. Gabizon, M. Mor, M. M. Rosenberg, L. Britan, Z. Hayouka, M. Kotler, D. E. Shalev, A. Friedler, *Biopolym. – Pept. Sci. Sect.* **2008**, *90*, 105–116.
[44] T. Goshen-Lago, A. Goldberg-Carp, D. Melamed, I. Darlyuk-Saadon, C. Bai, N. G. Ahn, A. Admon, D. Engelberg, *Mol. Biol. Cell* **2016**, *27*, 2771–2783.
[45] K. Smorodinsky-Atias, T. Goshen-Lago, A. Goldberg-Carp, A. Shir, N. Mooshayef, J. Beenstock, Y. Karamansha, I. Darlyuk-Saadon, O. Livnah, N. G. Ahn, A. Admon, D. Engelberg, *Mol. Biol. Cell* **2015**, *27*, 1026–1039.

Manuscript received: November 25, 2021
Accepted manuscript online: January 17, 2022
Version of record online: February 9, 2022